Medicine in Novel Technology and Devices 4 (2019) 100022

Contents lists available at ScienceDirect

Medicine in Novel Technology and Devices

journal homepage: www.journals.elsevier.com/medicine-in-novel-technology-and-devices/

Research Paper

Nano-hydroxyapatite(n-HA) involved in the regeneration of rat nerve injury triggered by overloading stretch

Meili Liu [a,b], Chongquan Huang [a,b], Zhijun Zhao [a,b], Anqing Wang [a,b], Ping Li [a,b], Yubo Fan [a,b,c,d], Gang Zhou [a,b,*]

[a] Key Laboratory for Biomechanics and Mechanobiology of Ministry of Education, School of Biological Science and Medical Engineering, Beihang University, Beijing, 100083, China
[b] Beijing Advanced Innovation Centre for Biomedical Engineering, Beihang University, Beijing, 102402, China
[c] Shenzhen Research Insititute of Beihang University, Beihang University, Shenzhen, 518057, China
[d] National Research Center for Rehabilitation Technical Aids, Beijing, 100176, China

ARTICLE INFO

Keywords:
Nano-hydroxyapatite(n-HA)
Mechanical stretch
Nerve injury
Netrin-1
Nerve regeneration

ABSTRACT

Damage of axon and glial scars formation both inhibit nerve regenerative growth during nerve injury. In addition, mechanical stretch at high displacement rates of 10% tensile strain can cause marked nerve injury, it is important for finding a proper nano biomaterial to repair nerve injury. Nano-hydroxyapatite (n-HA) has excellent biocompatibility and high bioactivity, which is a good candidate for biomedical engineering applications. But the certain mechanism of n-HA on the injured nerve is seldom reported. In this study, we determined the role of n-HA on the mechanical stretch-induced nerve injury at adult rat spine. Mechanical stretch under strain 10% at displacement rates of 60 mm/min can cause marked broken vessels and edema in spinal cord and dorsal root ganglion tissue in haematoxylin-eosin (HE) staining. However, n-HA application can reverse hemorrhage and edema triggered by high rates of 60 mm/min stretch. Moreover, n-HA can promote positive staining of Netrin-1 increase significantly in spinal cord and dorsal root ganglion tested by immunohistochemistry (IHC) staining. In general, our study indicated that n-HA can repair mechanical stretch-induced nerve injury, it may provide a new approach to block injury and accelerate nerve regeneration in future.

1. Introduction

Nerve injury is a major problem for the human health, which is related to the mechanical overloading stimulation, traumatic brain injury, low back pain and nervous tumor etc. [1–3] The damage of nerve in the central nervous system always produces glial scars, these inhibitory effects may prevent the regeneration of most nervous system [4]. Mechanical overloading can stimulate nerve injury depending on the magnitude of the mechanical stretch. Moreover, a relatively severe stretch (high tensile strain of 20% at 1 Hz) can result in significant neuronal injury [5,6]. It is difficult to repair for serious injury [7]. Thus, it is important to find a new approach for improving injured nerve regeneration.

In recent years, studies have shown that hydroxyapatite was applied in tissue engineering regeneration. Hydroxyapatite (HA, $Ca_{10}(PO_4)_6(OH)_2$) is an important inorganic component of biological bone tissues, because it has excellent biocompatibility, high bioactivity, and high thermal stability, which attracted much attention as an good candidate for biomedical engineering applications [8]. Nano-Hydroxyapatite (n-HA), due to their advantageous feature of a high surface-to-volume ratio, they could elicit a higher degree of biological plasticity compared with conventional micro-materials. n-HA has good mechanical properties and can be designed into a variety of forms, such as: biofilm, spinning, microtubes, etc. [9] In the past, the HA materials were mainly used in the hard tissue regeneration [10–13], but n-HA was also reported that it can promote the cortical neuronal outgrowth in our previous study which showed that n-HA can promote axonal guidance growth [14]. In a previous study, a growth conduit was adsorbed laminin onto the HA-coated tendon chitosan, it can repair the sciatic nerve of rats [15]. Recently, HA and type I collagen were made into hydrogels, was used to promote cell proliferation and repair the sciatic nerve of rats [16].

n-HA was also applied in tissue engineering. Oley Maximillian

* Corresponding author. Key Laboratory for Biomechanics and Mechanobiology of Ministry of Education, School of Biological Science and Medical Engineering, Beihang University, Beijing, 100083, China.
E-mail address: zhougang@buaa.edu.cn (G. Zhou).

https://doi.org/10.1016/j.mednotd.2019.100022
Received 8 November 2019; Received in revised form 19 November 2019; Accepted 26 November 2019

Christian et al. added a new additive, platelet-rich plasma (PRP), to the hydroxy carbonated apatite to make a scaffold material. Then they used this new scaffold material for the skull injury repair surgery in rats, and also achieved good results [17]. However, the above experiments have designed a composite material in which HA binds to the remaining growth factors/extracellular matrix, and the effect of HA itself on neuronal repair has not been reported. In our study, we established a model of spinal cord injury in rats by overloading mechanical stretch. And then we investigated the effect of n-HA on spinal cord and dorsal root ganglion (DRG) in injured spine. Then, we determined the expression of Netrin-1 in neurons. n-HA can well improve the nerve injury triggered by high magnitude of mechanical stretch. It will be a good candidate for the nerve regeneration.

2. Materials and methods

2.1. Ethics statement

All experiments involving the use of animals were following Provisions and General Recommendation of Chinese Experimental Animals Administration Legislation and were approved by Beijing Municipal Science & Technology Commission (Permit Number: SCXK (Beijing) 2006–0008 and SYXK (Beijing) 2006–0025).

2.2. Preparation of materials

n-HA was synthesized by precipitation method [18]. In briefly, calcium nitrate Ca $(NO_3)_2$) and trisodium Phosphate (Na_3PO_4) were dissolved in water, to prepare the HA crystals at a Ca/P molar ratio of 1.67. All the chemical reagents used in this work were analytic reagent (AR). Then the calcium solution was titrated into the phosphorous solution with vigorous stirring and the pH was adjusted to 10 by adding ammonia solution (NH_4·OH). In addition, reaction temperature was kept at 25 °C. After precipitation, the slurry was aging 24 h, and then centrifuged, washed with deionized water, and dried.

ALL the samples were weighted and dissolved in the culture maintained with modified Eagles' medium, 10% new born bovine serum, 5% D (+)- glucose, 50 IU/ml penicillin and 0.05 mg/ml streptomycin at 37 °C with 95% air and 5% CO_2. The solution was then sonicated for 1 h in a water bath. The final concentration of n-HA was 200 mg/ml, respectively.

2.3. Characterization of materials

2.3.1. X-ray diffractometry (XRD) analysis

XRD was used to determine the particle and crystallite size of the materials. These measurements were performed by Empyrean XRD analyzer (Cu-Kα) and PIXcel^{3D} detector from PANalytical Company. The samples were measured in the 2θ range from 5° to 70° (scan speed of 0.02° per second).

2.3.2. Fourier transform infrared (FT-IR) analysis

Chemical analysis of the complex was carried out by a FT-IR spectrophotometer (Thermo Nicolet 170SX) in the range from 500 cm^{-1} to 4000 cm^{-1} at 2 cm^{-1} resolution averaging 100 scans.

2.3.3. Transmission electron microscope (TEM) observation

The surface topography of n-HA particles was observed by TEM. TEM characterizations were used by a JME-100CX.

2.4. Mechanical stretch loading

All experiments were performed on freely moving adult male Wistar rats (Experimental Animal Center of Peking University Health Science Center, Beijing, China), weighing 200–300 g. The rats were housed in cages with free access to food and water, and maintained in a room temperature of 24 ± 2 °C with a 12-h light–dark cycle. Rats were anaesthetized by intraperitoneal pentobarbital (50 mg/kg) and were mounted on a stereotaxic instrument. A midline dorsal longitudinal incision was made over the lumbar spine. The paraspinal muscles were retracted and the L5 to S2 spine were clamped to stretch at Shimadzu Universal Testing Machine (TESTRESOURCES platform, Shimadzu, Japan) and displacement rates were controlled by Wintest software. The rat was placed on special test platform (Fig. 4), and displacement rates of 0.6 mm/min (St-0.6), 6 mm/min (St-6) and 60 mm/min (St-60) were applied on the L5 to S1 spine. All tensile strain were controlled under 10% in this test. All rats were stretched at a specific displacement rate only once.

2.5. n-HA treatment

After stretch, n-HA (200 mg/mL)was injected to the seriously mechanical stretch injured rats (St-60-*n*-HA),n-HA treated group was marked as n-HA + St in this study. All rats were housed for 14 days. All rats were observed for their walking pace and standing status during these days.

2.6. Haematoxylin & Eosin (H&E) staining

All the harvested spine and spinal dorsal root ganglion were laid flat on a small piece of card before immersing in 10% buffered formalin for fixation. This technique was used to avoid any artifact introduced in the tissue due to coiling of the nerve root when immersed in the fixation solution. After 72 h, the tissues were processed for H&E staining. Thin longitudinal paraffin sections of 5 μm thickness were stained and were examined under a light microscope (BX51, Olympus, Japan) and photographed using a digital camera system (DP2 analysis software, Olympus, Japan) attached to the microscope. The positive rate is the ratio of the number of positive particles to the total number of cells. The positive particles of Netrin-1 were counted in image J and analyzed in GraphPad Prism according to our previous methods [19].

2.7. Immunohistochemical staining (IHC)

To explore the Netrin-1 expression after mechanical stretch and n-HA treatment, sections were immune stained with goat anti- Netrin 1 antibody. Firstly, sections were deparaffinized in three changes of xylene for 5min, 2min and 2 min. Then sections were hydrated through graded alcohol from 100% to 70%, until into distilled water, sections were washed three times in distilled water, than washed in 2% Triton X in phosphate buffered saline (PBS, 3 times, 5min/time, 3 × 5 min), then treated with 3% H_2O_2 for 5–10 min to block endogenous peroxide activity, and then incubated with 5% normal horse serum to block nonspecific binding. Sections were then incubated with goat *anti*-Netrin-1 antibody (1:200) for 2 h or overnight at 4 °C. Sections were washed 3 times with PBS, then incubated with rabbit anti-goat HRP second antibody (1:200) for 2 h, then washed 3 times, all sections were incubated with DAB for 3–5 min, and then washed with PBS for 3 times, then sections were stained with haematoxylin for 30sec −3 min, then hydrated through graded alcohol from 50% to 100%, into xylene for 5 s. Finally, sections were cover slipped using neutral gum. Then stained sections were viewed under microscope (BX51, Olympus, Japan).

2.8. Statistical analysis

Data are given as means ± S.E.M. For statistical comparison, *t*-test or one-way ANOVA followed by Tukey's test was employed.*$p < 0.05$, **$p < 0.01$ and ***$p < 0.001$, were considered to be statistically significant.

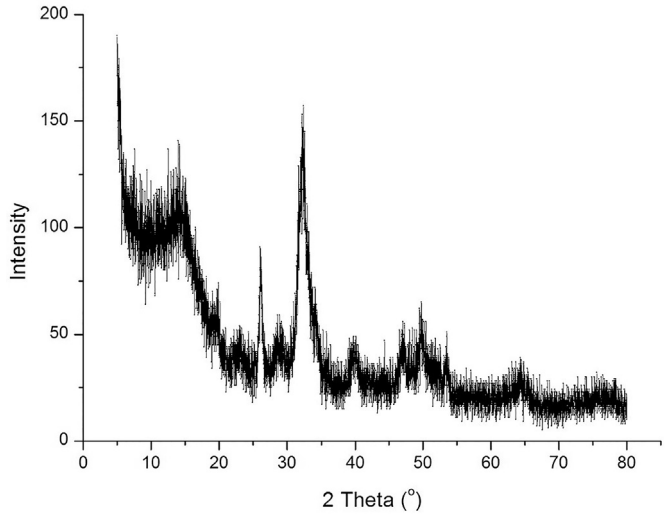

Fig. 1. XRD pattern of n-HA.

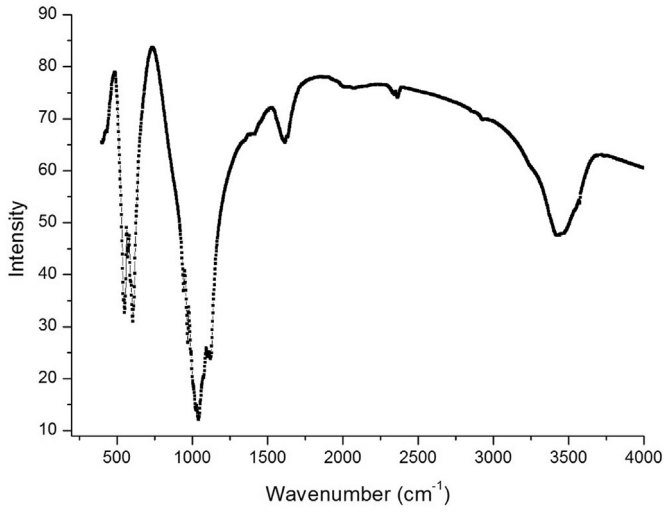

Fig. 2. IR spectrum of n-HA.

3. Results

3.1. XRD measurement

Fig. 1 described the X-ray diffraction pattern for the synthesized n-HA. All the diffraction peaks can be indexed as the hexagonal HA, located at 25.94°, 31.93°, 40.13°, 47.01° and 48.72° respectively. However, the broadening diffraction peaks indirectly prove that the synthetic n-HA was composed of small crystals that was belong to poorly crystalline and nonstoichiometric HA. Besides, according to XRD data calculated by Jade 9 software, the mean size of n-HA was about 24.21 ± 0.16 nm.

3.2. FT-IR analysis

The FT-IR analysis of n-HA samples (Fig. 2) showed the characteristic bands corresponding to hydroxyapatite. The broad bands extended from about 3000 cm^{-1}–3700 cm^{-1} and 1640 cm^{-1} corresponding to absorbed water. The shoulder at about 3571 cm^{-1} was attributed to the stretching vibration of the hydroxyl group (-OH). The strongest band at 1028–1109 cm^{-1} was assigned to the P–O stretching vibration of the phosphate groups (PO_4^{3-}). The weak band at about 489 cm^{-1} corresponds to the phosphate bending vibration. Also, the band at 564–609 cm^{-1} which

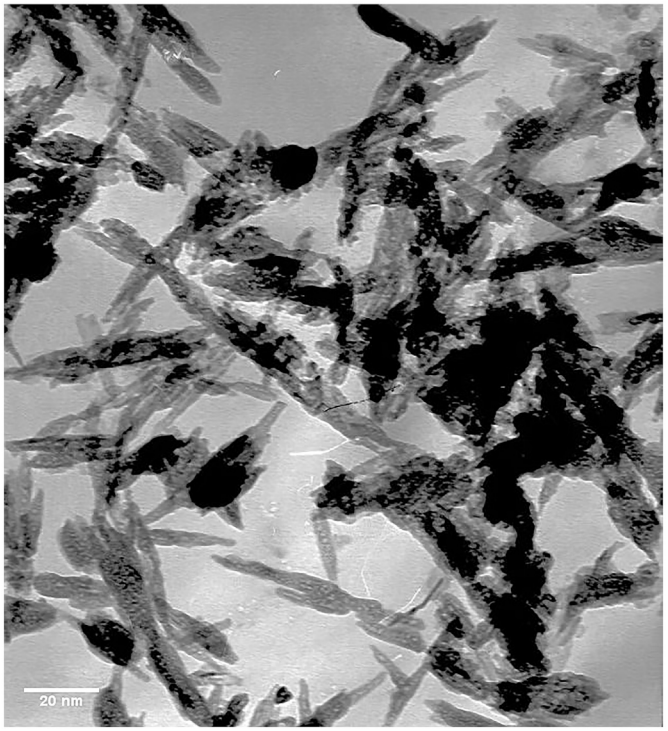

Fig. 3. TEM of n-HA Scale bar, 100 nm.

appears as a doublet was assigned to the PO_4^{3-} bending mode. The small bands of n-HA around 1425 cm^{-1} and 1464 cm^{-1} were ascribed to CO_3^{2-} ions, which indicated the formation was hydroxyapatite with carbonate (B-type) [19–21]. The presence of traces of CO_3^{2-} might arise from the subsequent sample handling steps, which improved the activity for inducing growth of neural cell.

3.3. TEM observation

For the n-HA (checked in Fig. 3), it was a needle shape, 4–5 nm in width and 20–30 nm in length from the TEM observations. The results of TEM observations agree with XRD data calculated.

3.4. Haematoxylin & Eosin (H&E) staining

In this study, all rats were subjected to mechanical loading in the TESTRESOURCES platform, which is showed in Fig. 4A. After mechanical stretch, all rats were housed for 14 days. We find that rats are in serious state after stretch for 1-day, individual rats occurred to death, but until the second day, rats became better to stand for drinking and feeding independently. Compared to the group of mechanical stretch at displacement rates of 60 mm/min (St-60), adding n-HA (200 mg/mL) can improve the status of rehabilitation. Spinal cord and dorsal root ganglion were harvested to observe its morphological changes after n-HA treatment. We determined those stretched rats by H& E staining, results showed that hemorrhage, broken vessels and edema occurred in spinal cord (Fig. 5A) and DRG (Fig. 5B) after mechanical stretch at displacement rates of 60 mm/min (St-60), but there are no significant changes after mechanical stretch at displacement rates of 0.6 mm/min (St-0.6), there is minor hemorrhage after mechanical stretch at displacement rates of 6 mm/min (St-6), as displacement rates increased, nerve injury is more obvious (Fig. 5). However, n-HA treatment can reduce hemorrhage induced by mechanical stretch at displacement rates of 60 mm/min (Fig. 5) in the morphological changes by HE staining.

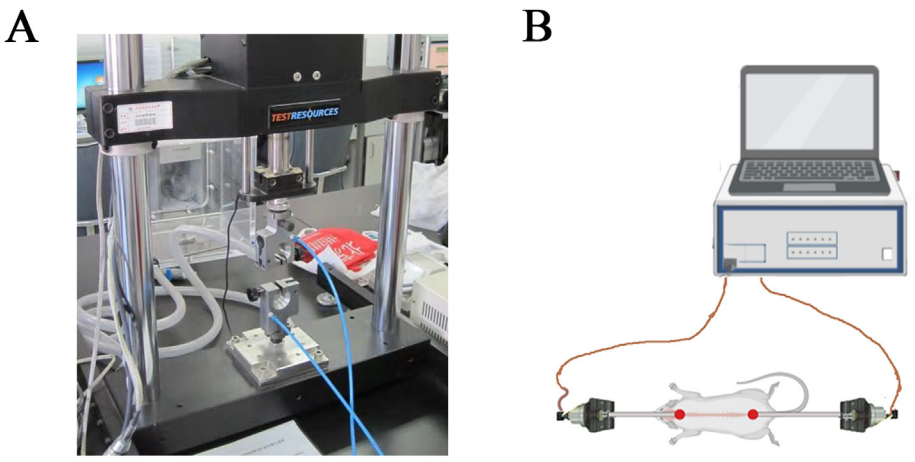

Fig. 4. TESTRESOURCES platform. A: Actual device with upper and lower two chucks connected to the power supply. B: Schematic diagram of stretching device.

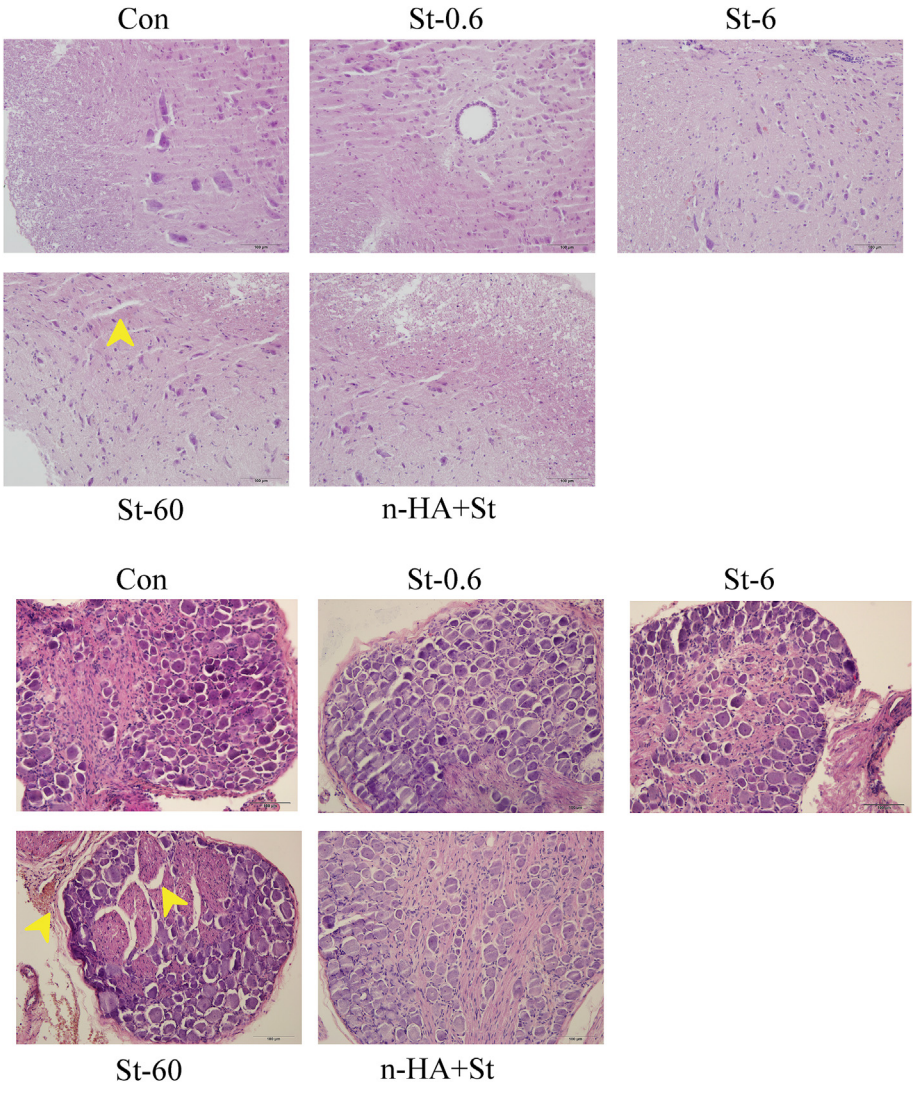

Fig. 5. Morphological changes of spinal cord and dorsal root ganglion in adult rat lumbar spinal nerve roots after mechanical stretch. Displacement rates of 0.6 mm/min (St-0.6), 6 mm/min (St-6) and 60 mm/min (St-60) were applied to L5 roots at pre-determined strain range <10%. Haematoxylin & Eosin staining results showed that hemorrhage, broken vessels and edema occurred in spinal cord and DRG after mechanical stretch at St-60 (Fig. 5A and B), and n-HA reversed stretch injury in spinal cord and DRG. The remarkable histopathology area were marked with yellow arrow.

3.5. Immunohistochemical staining (IHC)

All stretched rats were subjected to determine the axonal guidance cues for Netrin- 1 in the spinal cord and DRG by IHC staining. The percentage of positive Netrin 1 staining was determined by the ratio of the number of Netrin-1 positive cells over the total of 50 cells in one count. The average of 3 counts (in spinal cord slices) and the average of 5 counts (in DRG slices) were calculated as the percentage of Netrin-1 expression in a certain treatment (Fig. S1).

Our results showed that Netrin-1 positive staining increased

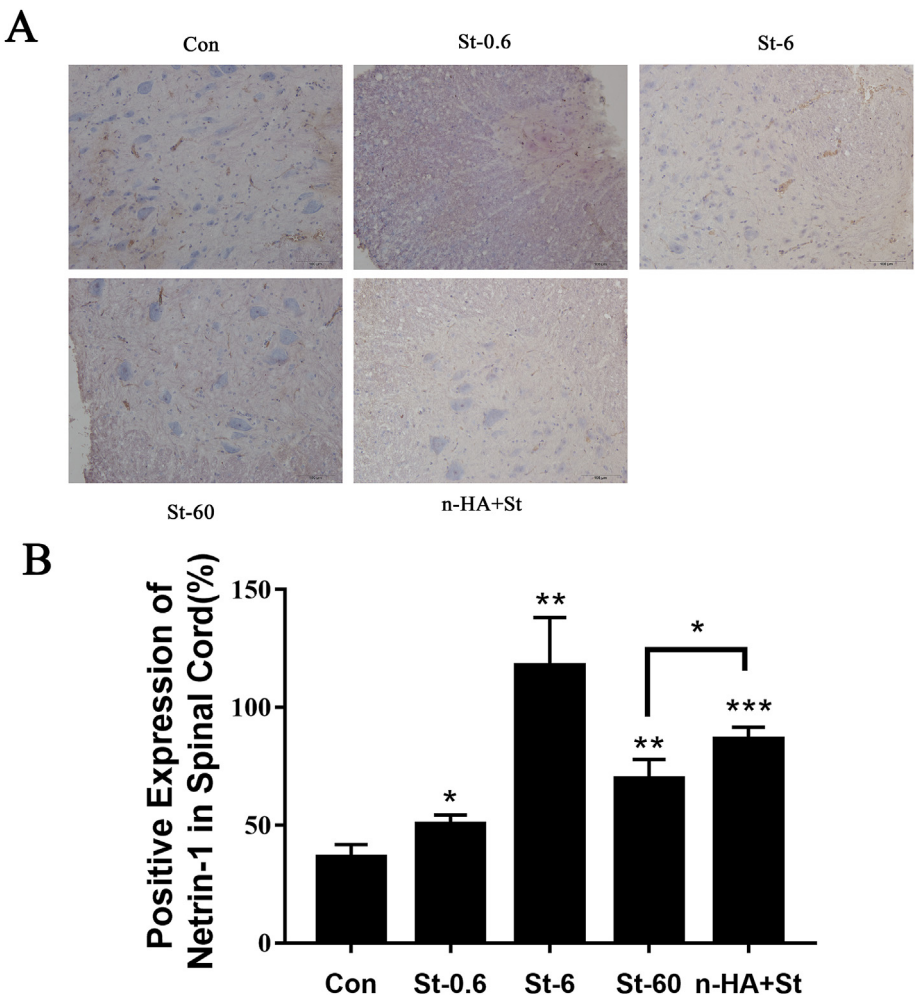

Fig. 6. Netrin-1 immunostaining in spinal cord neurons after mechanical stretch. Compared to control group, netrin-1 immune stained sections revealed Netrin-1 significant accumulation (Fig. 6A) after mechanical stretch at displacement rates of 0.6 mm/min (St-0.6), 6 mm/min (St-6) and 60 mm/min (St-60), statistical analysis results showed in Fig. 6B n-HA treatment increased the Netrin-1 expression in spinal cord. $^{**}p < 0.01$ and $^{***}p < 0.001$ were considered to be statistically significant.

significantly in spinal cord tissue slices, as mechanical stretch at displacement rates increased, Netrin-1 positive staining increased significantly in rat spinal cord (Fig. 6) (St-0.6, n = 3, t = 3.55, $p < 0.05$, St-6, n = 3, t = 6.64, $p < 0.01$; St-60, n = 3, t = 5.78, $p < 0.01$), and there is a significant increase of Netrin-1 expression in the group of n-HA treatment after mechanical stretch of displacement rate 60 mm/min (n-HA + St) (n = 3, t = 13.04, $p < 0.001$). More interestingly, there is a significant decrease of Netrin-1 expression at the group of St-60 compared to the group of St-6 (n = 3, t = 3.76, $p < 0.05$). And compared to the group of St-60, n-HA treatment enhanced the Netrin-1 expression (n = 3, t = 3.59, $p < 0.05$) (Fig. 6).

During mechanical stretch, axon can be affected significantly in DRG, we determined Netrin1 expression after mechanical stretch at displacement rates of 0.6 mm/min, 6 mm/min, 60 mm/min. There is significant increase of positive Netrin 1 staining in different treatment group (St-0.6, n = 5, t = 18.34, $p < 0.001$; St-6, n = 5, t = 26.52, $p < 0.001$; St-60, n = 5, t = 6.56, $p < 0.001$), while n-HA treatment can cause significant increase of positive Netrin1 staining (n = 5, t = 12.64, $p < 0.001$). In addition, there is a significant decrease of Netrin-1 expression at the group of St-60 compared to the group of St-6 (n = 5, t = 23.17, $p < 0.001$). And compared to the group of St-60, n-HA treatment enhanced the Netrin-1 expression (n = 5, t = 9.84, $p < 0.001$), results showed in Fig. 7.

4. Discussion

Previous study indicated that higher mechanical stretch may induce the damage of nervous system, and glia scar formation to inhibit the injured nerve regeneration [22,23]. Overloading mechanical stretch at displacement rates of 0.6 mm/min, 6 mm/min, and 60 mm/min all caused marked nerve injury in this study, as the magnitude increased to 60 mm/min, there is obvious hemorrhage, broken vessels and edema in morphological test. Thus, it can be used to establish a nerve injury model, which is consisted with previous study [5].

However, during tissue regeneration, the nano biomaterials were applied to repair injured tissues, for example, n-HA, and graphene etc. n-HA has a high surface-to-volume ratio and excellent bioactivity, which is often applied to bone tissue engineering. Besides, n-HA was attributed to their advantageous feature of Ca^{2+} and PO_4^{3-} played very important roles in the binding progress. n-HA was proposed a new microenvironment, which naturally mimics the structure of extracellular matrix (ECM). The selective guidance is possibly attributed to the change of calcium transient by n-HA stimulation. Hence the binding of calcium to the troponin [1], which communicates with the tropomyosin to undergo a conformational/rotation [24].

Some cellular molecular often lead neurons to grow towards target neurons during nerve regeneration and development. Netrin-1 is one of axonal guidance growth cues, which always response to different

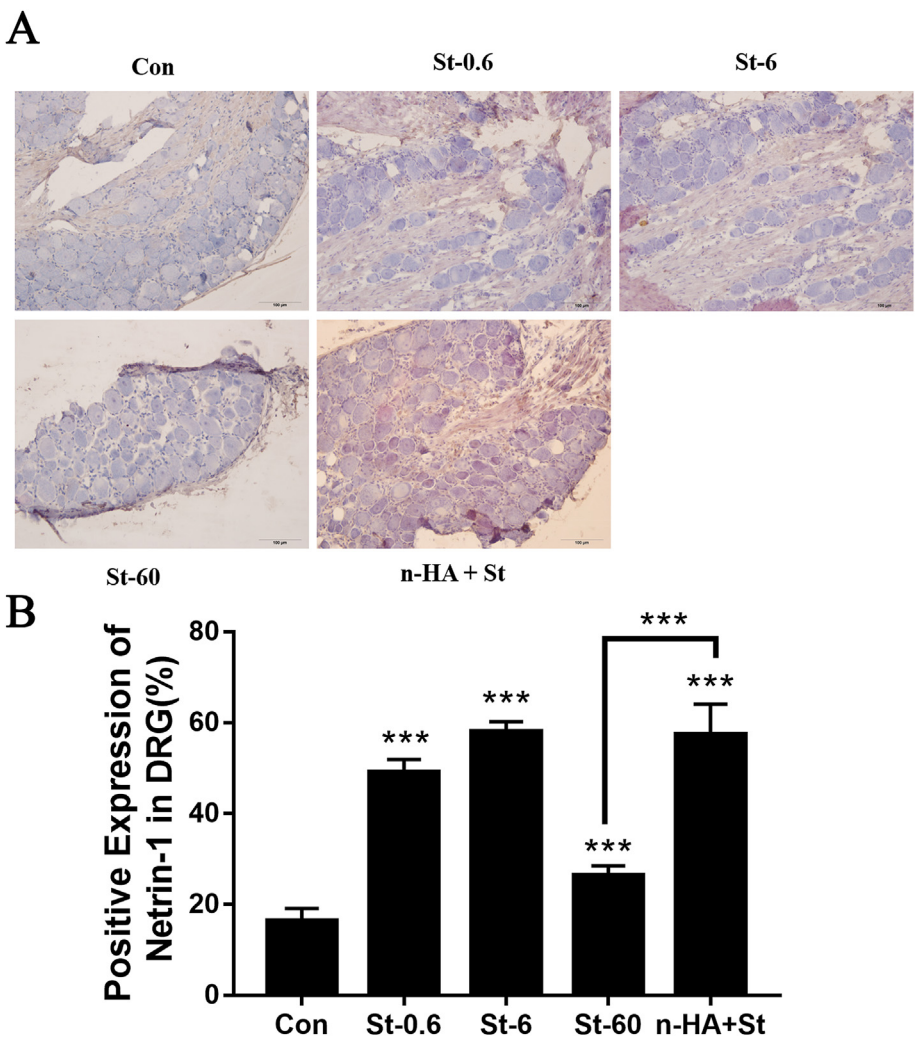

Fig. 7. Netrin-1 immunostaining in DRG neurons after mechanical stretch. Compared to control group, Netrin-1 immune stained sections revealed Netrin-1 significant accumulation (Fig. 7A) after mechanical stretch at displacement rates of 0.6 mm/min (St-0.6), 6 mm/min (St-6) and 60 mm/min (St-60), statistical analysis results showed in Fig. 7B n-HA treatment increased the Netrin-1 expression in DRG. $*p < 0.05$, $**p < 0.01$ and $***p < 0.001$ were considered to be statistically significant. Scale: 100 μm.

stimulation during nerve repairment [25,26]. In this study, we detected the Netrin-1 expression to clarify the n-HA role on injured nerve regeneration. We find that n-HA reversed the injury effect of higher mechanical stretch overloading, which increased the Netrin-1 expression to inhibit nerve injury in spinal cord and dorsal root ganglion tissue slice in immunohistochemistry assay. Our research also indicated the n-HA repair function, which is reported in bone, skin and nerves [13,15,27]. It is a promising material for regenerative medicine. Understanding the role of n-HA in neuronal repair is the first step, in the future we may also make n-HA in various forms and attach different types of growth factors or coatings to achieve a more beneficial repair effect after nerve injury.

5. Conclusion

Our study is an enhanced understanding the mechanisms of n-HA on repairing injured nerves triggered by higher mechanical stretch, which will reveal new approaches to repair the damaged nervous system and/or restore function.

Author contributions section

Liu Meili & Huang Chongquan: Writing - original draft, Writing - review & editing; Investigation; Methodology; Zhao Zhijun & Wang Anqing: Data curation; Investigation; Li Ping & Fan Yubo: Methodology; Zhou Gang: Writing - review & editing.

Acknowledgments

This study was supported by funds from the National Natural Science Foundation of China (NSFC) Research Grant (31971238, 51574246, 61871014, 11827803, 31771019), and National Key Research and Development Program (2016YFC1100704, 2016YFC1102203), and also supported by 111 Project (B13003), and International Joint Research Center of Aerospace Biotechnology and Medical Engineering, Ministry of Science and Technology, China.

Appendix A. Supplementary data

Supplementary data to this article can be found online at https://doi.org/10.1016/j.medntd.2019.100022.

References

[1] Boukany PE, Morss A, Liao WC, Henslee B, Jung H, Zhang X, Yu B, Wang X, Wu Y, Li L, Gao K, Hu X, Zhao X, Hemminger O, Lu W, Lafyatis GP, Lee LJ. Nanochannel electroporation delivers precise amounts of biomolecules into living cells. Nat Nanotechnol 2011;6(11):747–54. https://doi.org/nnano.2011.164.

[2] Hartvigsen J, Hancock MJ, Kongsted A, Louw Q, Ferreira ML, Genevay S, Hoy D, Karppinen J, Pransky G, Sieper J, Smeets RJ, Underwood M, Workin LLBPS. What low back pain is and why we need to pay attention. Lancet 2018;391(10137):2356–67. https://doi.org/10.1016/S0140-6736(18)30480-X.

[3] Hoy D, March L, Brooks P, Blyth F, Woolf A, Bain C, Williams G, Smith E, Vos T, Barendregt J, Murray C, Burstein R, Buchbinder R. The global burden of low back pain: estimates from the Global Burden of Disease 2010 study. Ann Rheum Dis 2014;73(6):968–74. https://doi.org/10.1136/annrheumdis-2013-204428.

[4] Fawcett JW, Asher RA. The glial scar and central nervous system repair. Brain Res Bull 1999;49(6):377–91. https://doi.org/10.1016/s0361-9230(99)00072-6.
[5] Gladman SJ, Ward RE, Michael-Titus AT, Knight MM, Priestley JV. The effect of mechanical strain or hypoxia on cell death in subpopulations of rat dorsal root ganglion neurons in vitro. Neuroscience 2010;171(2):577–87. https://doi.org/10.1016/j.neuroscience.2010.07.009.
[6] Magou GC, Pfister BJ, Berlin JR. Effect of acute stretch injury on action potential and network activity of rat neocortical neurons in culture. Brain Res 2015;1624:525–35. https://doi.org/10.1016/j.brainres.2015.07.056.
[7] Pfister BJ, Huang JH, Kameswaran N, Zager EL, Smith DH. Neural engineering to produce in vitro nerve constructs and neurointerface. Neurosurgery 2007;60(1):137–41. https://doi.org/10.1227/01.NEU.0000249197.61280.1D. discussion 141-2.
[8] Chen F, Huang P, Zhu YJ, Wu J, Zhang CL, Cui DX. The photoluminescence, drug delivery and imaging properties of multifunctional Eu3+/Gd3+ dual-doped hydroxyapatite nanorods. Biomaterials 2011;32(34):9031–9. https://doi.org/10.1016/j.biomaterials.2011.08.032.
[9] Liao JG, Li YQ, Duan XZ, Zhu LL. Nano-hydroxyapatite/polymer composite as bone repair materials. Prog Chem 2015;27(2–3):220–8. https://doi.org/10.7536/Pc140810.
[10] Wang H, Li Y, Zuo Y, Li J, Ma S, Cheng L. Biocompatibility and osteogenesis of biomimetic nano-hydroxyapatite/polyamide composite scaffolds for bone tissue engineering. Biomaterials 2007;28(22):3338–48. https://doi.org/10.1016/j.biomaterials.2007.04.014.
[11] Sun TW, Zhu YJ, Chen F, Zhang YG. Ultralong hydroxyapatite nanowire/collagen biopaper with high flexibility, improved mechanical properties and excellent cellular attachment. Chem Asian J 2017;12(6):655–64. https://doi.org/10.1002/asia.201601592.
[12] Sun TW, Zhu YJ, Chen F. Highly flexible multifunctional biopaper comprising chitosan reinforced by ultralong hydroxyapatite nanowires. Chemistry 2017;23(16):3850–62. https://doi.org/10.1002/chem.201605165.
[13] Liao J, Li Y, Li H, Liu J, Xie Y, Wang J, Zhang Y. Preparation, bioactivity and mechanism of nano-hydroxyapatite/sodium alginate/chitosan bone repair material. J Appl Biomater Funct Mater 2018;16(1):28–35. https://doi.org/10.5301/jabfm.5000372.
[14] Liu M, Zhou G, Song W, Li P, Liu H, Niu X, Fan Y. Effect of nano-hydroxyapatite on the axonal guidance growth of rat cortical neurons. Nanoscale 2012;4(10):3201–7. https://doi.org/10.1039/c2nr30072a.
[15] Itoh S, Yamaguchi I, Suzuki M, Ichinose S, Takakuda K, Kobayashi H, Shinomiya K, Tanaka J. Hydroxyapatite-coated tendon chitosan tubes with adsorbed laminin peptides facilitate nerve regeneration in vivo. Brain Res 2003;993(1–2):111–23. https://doi.org/10.1016/j.brainres.2003.09.003.
[16] Salehi M, Naseri-Nosar M, Ebrahimi-Barough S, Nourani M, Vaez A, Farzamfar S, Ai J. Regeneration of sciatic nerve crush injury by a hydroxyapatite nanoparticle-containing collagen type I hydrogel. J Physiol Sci 2018;68(5):579–87. https://doi.org/10.1007/s12576-017-0564-6.
[17] Oley MC, Islam AA, Hatta M, Hardjo M, Nirmalasari L, Rendy L, Ana ID, Bachtiar I. Effects of platelet-rich plasma and carbonated hydroxyapatite combination on cranial defect Bone Regeneration: an animal study. Wound Med 2018;21:12–5. https://doi.org/10.1016/j.wndm.2018.05.001.
[18] Han Y, Xu K, Lu J. Morphology and composition of hydroxyapatite coatings prepared by hydrothermal treatment on electrodeposited brushite coatings. J Mater Sci Mater Med 1999;10(4):243–8. https://doi.org/10.1023/a:1008914330004.
[19] Huang Y, Zhou G, Zheng L, Liu H, Niu X, Fan Y. Micro-/nano- sized hydroxyapatite directs differentiation of rat bone marrow derived mesenchymal stem cells towards an osteoblast lineage. Nanoscale 2012;4(7):2484–90. https://doi.org/10.1039/c2nr12072k.
[20] Lee SJ, Yoon YS, Lee MH, Oh NS. Nanosized hydroxyapatite powder synthesized from eggshell and phosphoric acid. J Nanosci Nanotechnol 2007;7(11):4061–4. https://doi.org/10.1166/jnn.2007.067.
[21] Stanic V, Janackovic D, Dimitrijevic S, Tanaskovic SB, Mitric M, Pavlovic MS, Krstic A, Jovanovic D, Raicevic S. Synthesis of antimicrobial monophase silver-doped hydroxyapatite nanopowders for bone tissue engineering. Appl Surf Sci 2011;257(9):4510–8. https://doi.org/10.1016/j.apsusc.2010.12.113.
[22] Laplaca MC, Prado GR. Neural mechanobiology and neuronal vulnerability to traumatic loading. J Biomech 2010;43(1):71–8. https://doi.org/S0021-9290(09)00502-8.
[23] Slemmer JE, Zhu C, Landshamer S, Trabold R, Grohm J, Ardeshiri A, Wagner E, Sweeney MI, Blomgren K, Culmsee C, Weber JT, Plesnila N. Causal role of apoptosis-inducing factor for neuronal cell death following traumatic brain injury. Am J Pathol 2008;173(6):1795–805. https://doi.org/S0002-9440(10)61563-5.
[24] Clusin WT. Mechanisms of calcium transient and action potential alternans in cardiac cells and tissues. Am J Physiol Heart Circ Physiol 2008;294(1):H1–10. https://doi.org/00802.2007.
[25] Junge HJ, Yung AR, Goodrich LV, Chen Z. Netrin1/DCC signaling promotes neuronal migration in the dorsal spinal cord. Neural Dev 2016;11(1):19. https://doi.org/10.1186/s13064-016-0074-x.
[26] Varadarajan SG, Butler SJ. Netrin1 establishes multiple boundaries for axon growth in the developing spinal cord. Dev Biol 2017;430(1):177–87. https://doi.org/10.1016/j.ydbio.2017.08.001.
[27] Okabayashi R, Nakamura M, Okabayashi T, Tanaka Y, Nagai A, Yamashita K. Efficacy of polarized hydroxyapatite and silk fibroin composite dressing gel on epidermal recovery from full-thickness skin wounds. J Biomed Mater Res B Appl Biomater 2009;90(2):641–6. https://doi.org/10.1002/jbm.b.31329.